



Short-Term Administration of Astaxanthin Attenuates Retinal Changes in Diet-Induced Diabetic *Psammomys obesus*

Basma Baccouche, Maha Benlarbi, Alistair J. Barber & Rafika Ben Chaouacha-Chekir

To cite this article: Basma Baccouche, Maha Benlarbi, Alistair J. Barber & Rafika Ben Chaouacha-Chekir (2018): Short-Term Administration of Astaxanthin Attenuates Retinal Changes in Diet-Induced Diabetic *Psammomys obesus*, Current Eye Research, DOI: [10.1080/02713683.2018.1484143](https://doi.org/10.1080/02713683.2018.1484143)

To link to this article: <https://doi.org/10.1080/02713683.2018.1484143>



Published online: 20 Jul 2018.



Submit your article to this journal [↗](#)



Article views: 1



View Crossmark data [↗](#)



Short-Term Administration of Astaxanthin Attenuates Retinal Changes in Diet-Induced Diabetic *Psammomys obesus*

Basma Baccouche^{a,b}, Maha Benlarbi^a, Alistair J. Barber^c, and Rafika Ben Chaouacha-Chekir^a

^aLaboratoire de Physiopathologies, Alimentations et Biomolécules (PAB), Institut Supérieur de Biotechnologie de Sidi Thabet (ISBST), Univ Manouba (UMA), BiotechPole Sidi Thabet, Ariana, Tunisie; ^bFaculté des Sciences de Bizerte (FSB), Université de Carthage (UCAR), Tunis, Tunisie; ^cDepartment of Ophthalmology, Penn State Hershey Eye Center, Milton S. Hershey Medical Center, Penn State College of Medicine, Hershey, PA, USA

ABSTRACT

Objectives: *Psammomys obesus* is a high-fat diet (HFD)-fed animal model of obesity and type 2 diabetes recently explored as a model of non-proliferative diabetic retinopathy. This study tested the protective effect of the pigment astaxanthin (AST) in the *P. obesus* diabetic retina.

Methods: Young adult *P. obesus* were randomly assigned to two groups. The control group received a normal diet consisting of a plant-based regimen, and the HFD group received an enriched laboratory chow. After 3 months, control and diabetic rodents were administered vehicle or AST, daily for 7 days. Body weight, blood glucose, and plasma pentosidine were assessed. Frozen sections of retinas were immunolabeled for markers of oxidative stress, glial reactivity and retinal ganglion cell bodies, and imaged by confocal microscopy.

Results: Retinal tissue from AST-treated control and HFD-diabetic *P. obesus* showed a greater expression of the antioxidant enzyme heme oxygenase-1 (HO-1). In retinas of HFD-diabetic AST-treated *P. obesus*, cellular retinaldehyde binding protein and glutamine synthetase in Müller cells were more intense compared to the untreated HFD-diabetic group. HFD-induced diabetes downregulated the expression of glial fibrillary acidic protein in astrocytes, the POU domain protein 3A in retinal ganglion cells, and synaptophysin throughout the plexiform layers.

Discussion: Our results show that type 2-like diabetes induced by HFD affected glial and neuronal retinal cell homeostasis. AST treatment induced the antioxidant enzyme HO-1 and reduced glial reactivity. These findings suggest that diabetic *P. obesus* is a useful model of HFD-induced obesity and diabetes to evaluate early neuroglial retinal alterations and antioxidant neuroprotection mechanisms in DR.

ARTICLE HISTORY

Received 8 January 2018

Revised 22 May 2018

Accepted 28 May 2018

KEYWORDS

Diabetic retinopathy; high-fat diet; oxidative stress; neurodegeneration; neuroprotection

Introduction

Over the last 50 years, our eating habits have undergone rapid nutritional transitions related to profound economic and social changes.¹ Physical inactivity and consumption of low-fiber processed food, relatively rich in fat and with a high glycemic index, created a significant imbalance between calorie intake and energy expenditure, resulting in an increase in prevalence of weight gain or obesity.¹ The global endemic of obesity partly explains the dramatic increase in the incidence and prevalence of type 2 diabetes (T2D) over the past 20 years.^{2–5} Common complications associated with T2D include chronic kidney disease (diabetic nephropathy), peripheral nerve damage (diabetic neuropathy), and vision loss leading to irreversible blindness [diabetic retinopathy (DR)].

The non-proliferative diabetic retinopathy (NPDR) at early stages is not severe enough for patients to notice any of the classic symptoms.⁶ Before the onset of vascular lesions, diabetes-induced retinal pathology includes a number of alterations in glutamate metabolism, growth factor signal transduction, and increased cell death, glial reactivity, elevated inflammatory signals, reduction in synaptic protein, and

elevated oxidative stress.^{7–10} Progressive inner retinal thinning is also established to occur in both humans and animal models, indicating neurodegenerative changes that are likely to impact visual function.^{11,12} Since more than 20% of T2D patients are diagnosed with DR at the time of first diagnosis of diabetes, it has become important to identify new animal models of T2D and study the early features of retinal pathology in those models.^{13–15}

Desert gerbils are high-fat diet (HFD) models naturally prone to diet-induced metabolic syndrome and T2D.^{16–19} The herbivorous and diurnal sand rat *Psammomys obesus* is endemic to the North African and Middle East regions.^{20,21}

As an arid-adapted gerbil, *P. obesus* has a low metabolic rate and is able to meet its energy demand by consuming large amounts (up to 80% of its body mass) of halophytic Chenopodiaceae plant (*Atriplex halimus*, *Salsola foetida*; 0.4 kcal/g).^{22–25} When exposed under laboratory conditions to a standard laboratory chow (2.93–3.25 kcal/g)^{26–30} or to an enriched diet (3.7–4 kcal/g),^{31,32} *P. obesus* develops chronic hyperglycemia, insulin and leptin resistance, obesity, dyslipidemia, hepatic and intestinal metabolism dysfunction,

myocardial anomalies, and renal failure. Therefore, *P. obesus* can be used as a model of T2D when placed on an HFD.³³

Studies of phenotypic and functional characteristics of the *P. obesus* retina have described the photoreceptor specialization and a predominant cone function and structure.^{34,35} Electroretinogram (ERG) measurements revealed that cone-mediated function of *P. obesus* shares several features with that of human subjects^{35,36} and that retinal function and S-cone photoreceptors were particularly affected in 7-month diabetic *P. obesus*,^{36,37} suggesting the retina of these animals has features found in diabetic human retina that are not provided by other rodent models.^{34,35,38–40}

There is a growing interest in using micronutrition and antioxidant nutritional supplements in the treatment of diabetes-related complications. Carotenoids are a group of naturally and widely occurring pigments involved in promoting health vision. The xanthophyll astaxanthin (AST) is a red carotenoid that is synthesized by microorganisms and present in seafood, which has engendered interest related to its potential health benefits. In this study, we analyzed the retina morphology of 13-week diabetic *P. obesus* and attempt to address the potential protective impact of short-term (7-day) AST treatment on glial and neuronal alterations.

Materials and methods

Animals

P. obesus were captured in BOUHEDMA Park, Sidi Bouzid, a semidesert region of Tunisia. The animals were transferred to the animal facility of the Higher Institute of Biotechnology of Sidi-Thabet. Animal capture and experimentation were consistent with the Tunisian General Directorate of Forestry laws and approved by Tunisian Ministry of Agriculture (number of approval: 2012-2016/2214-1693). Animal experimentation was also consistent with the ARVO Statement for the ethical use of Animals in Ophthalmic and Vision Research and the local ethics committee of the Pasteur Institute of Tunis, Tunisia (2016/11/E/ISBST/V0). The animals were held in quarantine for acclimation and fed a natural diet (ND) composed of halophilic plants.^{20,41}

Diet and AST treatment

Male *P. obesus* between 3 and 4 months old were randomly assigned to two groups ($n = 8$). In accordance with previous studies,^{26,27,37,42,43} the control group was fed with a plant-based diet (Chenopodiaceae, *A. halimus*), rich in water (>80%) and mineral salts.^{26,41} The HFD group received a standard laboratory chow (containing 4% fat; 43% carbohydrates) supplemented as previously (+16% fat, 10% carbohydrates),^{32,44,45} and saline water (NaCl 0.9%). Animals were weighed every week. Blood was collected by retro-orbital sinus puncture at baseline and once a month during the HFD treatment. Blood glucose was estimated using an Accu-Check Blood Glucose Meter (Roche, Mannheim, Germany). The animals were housed at $25 \pm 2^\circ\text{C}$ with 12/12 h light/dark photoperiod and free access to food and water. After 12 weeks, *P. obesus* with blood glucose levels ≥ 8.3 mmol/L^{33,46–49} were classified as diabetic.

Control and diabetic rodents were randomly segregated into four groups ($n = 4$ per group) and were treated with either vehicle (water) or AST ($\geq 97\%$, Sigma-Aldrich, France), 10 mg/kg daily for 7 days by mouth using a gavage needle. AST dose was selected in consideration of previous reports.^{50,51} Animal treatment and AST administration were performed in the animal facility of the Higher Institute of Biotechnology of Sidi-Thabet.

Retinal tissue and plasma collection

At the end of the 13-week feeding regimen, gerbils were anesthetized (120 mg/kg ketamine) and sacrificed by decapitation at the Higher Institute of Biotechnology of Sidi-Thabet. For each animal, eyes were enucleated, prefixed in 4% paraformaldehyde (Sigma) in phosphate-buffered saline (PBS) 0.01 M for 45 min at room temperature. Ocular globes were dissected under binocular microscope. The anterior part of the eye (lens and cornea) was discarded. After removing the vitreous, the eye cups were oriented along the dorsoventral axis in molds filled with optimum cutting temperature (Tissue Tek), snap-frozen, and stored at -80°C .

Plasma samples were collected at the end of the experimentation from the control ($n = 3$) and diabetic ($n = 3$) in heparin-coated tubes, then centrifuged for 10 min at 5,000 rpm at 4°C . Plasma was carefully transferred, snap-frozen in liquid nitrogen, and immediately stored in -80°C until needed.

Determination of plasma pentosidine levels by high-performance liquid chromatography (HPLC)

Plasma sample preparation

Plasma pentosidine purification was performed as described previously.^{52,53} *P. obesus* plasma samples (35 μl each) were hydrolyzed by 6 M hydrochloric acid (HCl) for 18 h at 110°C . The samples were applied to SPE columns (6 cc Oasis MCX, France) and eluted by 5% ammonia in methanol. After evaporation to dryness under a stream of nitrogen gas, residue was resolubilized in 200 μl of 25 mM citric acid solution, then filtered through 0.45 μm Uptidisc PTFE.

HPLC assays

Ten microliters of the solution was injected in the UltiMate 3000 HPLC systems (Thermo Scientific, France) using Acclaim 120 C18 columns for reversed-phase separation (Thermo Scientific, France), maintained at 25°C and a flow rate of 1 ml/min. Standard pentosidine (Sigma, France) was used to obtain a standard curve. We used a trifluoroacetic acid (solvent A)/acetonitrile (solvent B) mobile phase. Gradient separation was performed by changing the proportions of the two solvents: gradient starts at 5% of solvent B, changes after 2 min to 95% solvent B for 20 min. The eluate was monitored by its fluorescence at 325/385 nm.

Immunohistochemistry

Retinal sections (10 μm thick) were collected on microscope slides (Fisher SuperfrostPlus) and stored in -80°C until

needed. Cryosections were permeabilized with 0.1% triton X-100 (Sigma) in PBS 0.01 M and incubated for 1 h in blocking buffer (10% normal donkey serum in 0.1% triton X-100 and PBS). Sections were incubated overnight at 4°C with primary monoclonal and polyclonal antibodies. Cellular retinaldehyde binding protein (CRALBP) (1:100, Santa Cruz Biotechnology, USA), glutamine synthetase (GS) (1:1500, Merk Millipore, USA), Synaptophysin Svp 38 (1:50, Sigma-Aldrich, USA), glial fibrillary acidic protein (GFAP) (1:2, EP672Y, Roche), heme oxygenase-1 (HO-1) (1:100, Abcam, USA), and brain-specific homeobox/POU domain protein 3A (Brn3a) (1:70, Santa Cruz Biotechnology, USA) were diluted in blocking buffer. Sections were washed two times for 15 min and incubated for 1 h at room temperature with secondary antibodies anti-mouse, anti-rabbit, and anti-goat, coupled with CY3, Alexa 488 or Alexa 594, respectively (Jackson ImmunoResearch, USA). Cell nuclei were counterstained with 10 µg/ml Hoechst® 33342 (Sigma).

Image capture and analysis

Fluorescence imaging was performed by confocal microscopy (Leica TCS SP8) in the Penn State College of Medicine Imaging Core Facility. Adobe Photoshop (San Diego, CA, USA) was used to create the final montages.

Cell layer thickness and number of nuclei per layer were calculated within a standard rectangle placed across captured images, equivalent to an area measuring 0.07 mm.^{2,37} The number of ganglion cells in the retinal nerve fiber layer (RNFL)/retinal ganglion cell layer (RGCL), and the number of cell nuclei in the inner nuclear layer (INL) and outer nuclear layer (ONL) were determined in the mid-peripheral region in retina (1–3 sections) of AST-treated and non-treated diabetic and control animals using Image J. Three to four animals were analyzed from each of the four treatment groups. Cell body densities were determined by converting micrographs to grayscale images. After applying a threshold, cell nuclei were separated by the “Watershed” function.⁵⁴ Layers of interest were selected and cells with more than 30 µm² were counted. Thickness of RGCL, inner/outer nuclear and plexiform layers was also measured using Image J.

CRALBP immunoreactivity was quantified with Image J. The micrographs were split into different channels and each channel was converted to grayscale images, a threshold was set, and fluorescent signal calculated.⁵⁵ The results, in arbitrary units, were mean gray values of the channel of interest.

Statistical analyses

Data are expressed as mean ± standard error of the mean (SEM). Statistical comparisons between the four groups were made by analysis of variance with Tukey multiple comparisons testing where appropriate. Student’s *t*-test was used to compare body weight, blood glucose, and plasma pentosidine level between the control and diabetic group (GraphPad Prism 6, GraphPad Software, Inc., La Jolla, CA, USA). The values were considered to be significantly different when $p \leq 0.05$.

Results

HFD induces diabetes in *P. obesus*

When maintained in captivity for 13 weeks, control animals given ND did not develop obesity (126.58 ± 3.38 g) or hyperglycemia (5.05 ± 0.50 mmol/l) (Figure 1A, B). Within 4 weeks, however, animals fed HFD gained significant body weight (+27.76%, $p \leq 0.05$) and developed hyperglycemia (9.75 ± 1.63 mmol/l, $p \leq 0.05$) in accordance with previous results.^{21,33} After 13 weeks, the HFD group developed obesity (+73.19%, $p \leq 0.001$) and significantly higher blood glucose (17.28 ± 1.61 mmol/l, $p \leq 0.001$) compared to controls. No difference in weight or blood glucose level was observed between control and diabetic groups after administration of AST.

HFD-induced diabetes promotes plasma pentosidine levels

Plasma pentosidine concentrations were markedly increased ($p \leq 0.05$) in 13-week diabetic animals (914 ± 88.39 pg/ml) compared to the controls (229 ± 88.26 pg/ml).

General retinal morphology and cell count

There was no noticeable difference in overall morphology between the control and HFD *P. obesus* retina

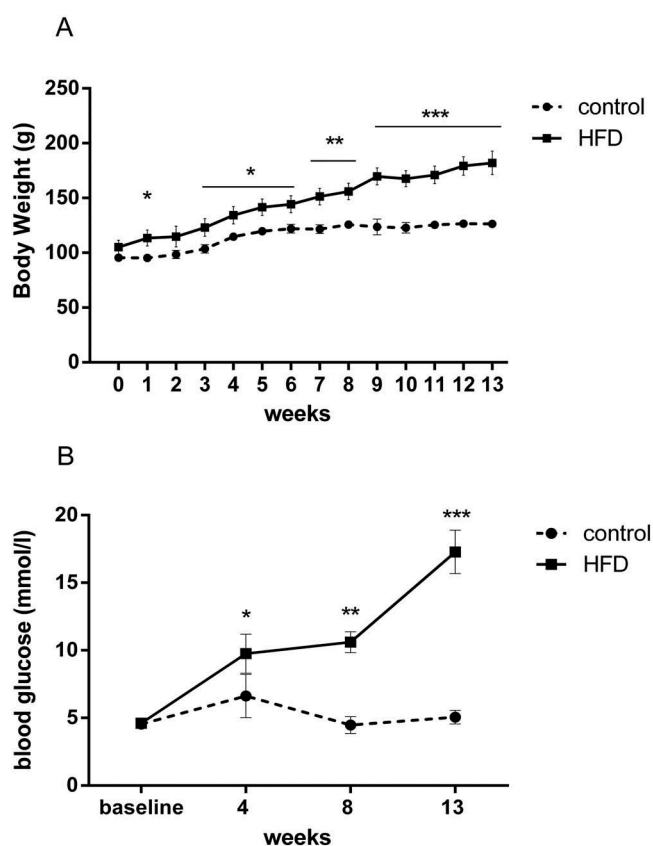


Figure 1. High-fat diet (HFD)-induced obesity and diabetes in *Psammomys obesus* fed for 13 weeks with either a natural diet (control) or an HFD. (A) Animals subjected to HFD developed increased body weight. (B) Blood glucose levels were significantly higher in HFD-diabetic animals compared to controls. Data are expressed as means ± SEM ($n = 8$). * $p < 0.05$, ** $p < 0.01$, *** $p < 0.001$.

(Figure 2A). Cell nuclei in the RGCL, INL, and ONLs were counted in controls and 13-week diabetic, treated and untreated retinas (Figure 2B). There was no significant difference in number of nuclei in the RGCL between control and hyperglycemic retinas. The number of nuclei in the INL was significantly reduced in diabetic animals but no significant change was detected in the number of nuclei in the ONL. No detectable change was noted in the

RGCL + IPL, INL, ONL, and OPL between control and diabetic groups (Figure 2C).

Astaxanthin promotes HO-1 expression

The expression of the oxidative stress marker HO-1 was examined using immunofluorescent microscopy (Figure 3). In control sections, HO-1 immunofluorescence was abundant,

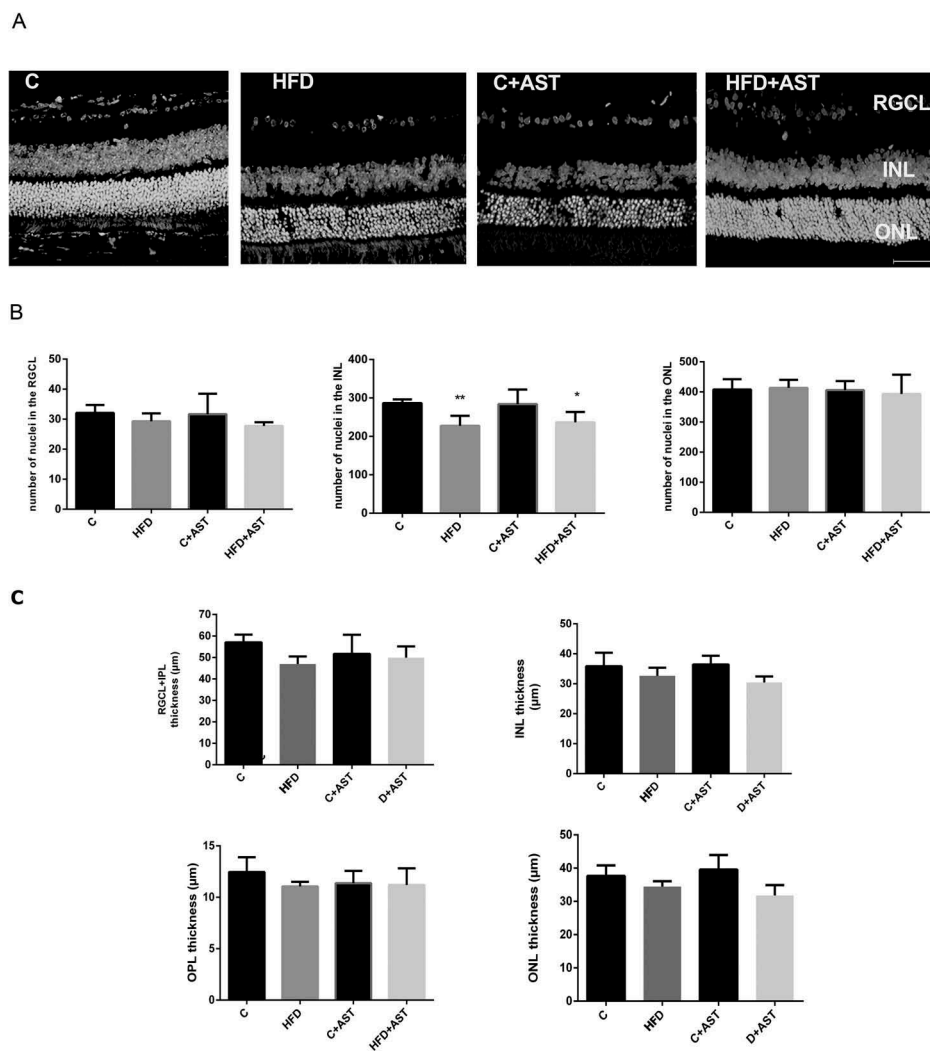


Figure 2. Retinal morphology and cell count. (A) Representative images of retinal layers revealed by nuclear staining (Hoechst). (B) Number of nuclei in the RGCL and ONL were not changed in diabetic *P. obesus* in comparison with lean animals. INL cell bodies decreased significantly in 13-week HFD-diabetic animals. (C) There was no significant difference in retinal thickness layers between diabetic and controls. * $p < 0.05$, ** $p < 0.01$.

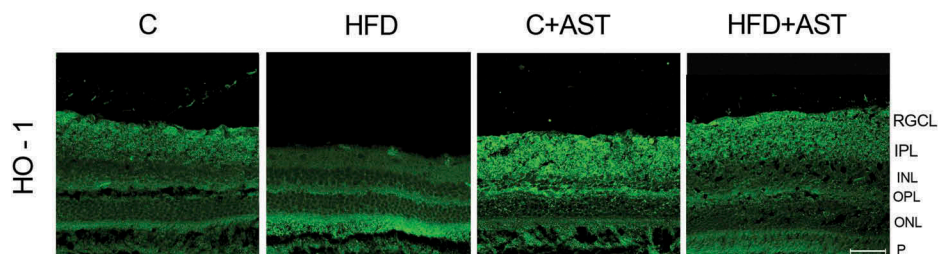


Figure 3. Representative micrographs of retinal sections stained using an anti-HO-1 antibody in C, control; HFD, HFD-diabetic gerbils; C + AST, control treated with AST; HFD + AST, HFD-diabetic treated with AST. AST treatment elevated the HO-1 expression in RGC and P layers in control and 3 months HFD-diabetic retinas. RGCL, retinal ganglion cell layer; INL, inner nuclear layer; ONL, outer nuclear layer; P, photoreceptor layer. Bar: 50 µm.

especially in the RGCL and IPL, whereas in the HFD-diabetic retinas HO-1 immunofluorescence was diminished in the IPL and more intense in the photoreceptor inner and outer segments. The retinas from the C + AST and HFD + AST groups also had greater HO-1 immunofluorescence intensity detected in the GCL, IPL, and OPL.

Astaxanthin short-term treatment attenuates glial dysfunction in the diabetic retina of *P. obesus*

To evaluate the progression of astrocyte and Müller cell reactivity, GFAP immunoreactivity was investigated. Immunofluorescence was abundant in the astrocytes of the retinas from control animals, appearing as a monolayer of projections in the inner limiting membrane and surrounding large blood vessels (Figure 4). There was reduced intensity of GFAP immunofluorescence in the astrocytes of the HFD-diabetic group compared to controls. The C + AST group had similar GFAP immunofluorescence intensity compared to untreated controls, as did the HFD + AST group. There was no detectable expression of GFAP in Müller cells in any of the treatment groups.

CRALBP and GS were also used as selective markers of retinal Müller cells.⁵⁶ In control animals, CRALBP was expressed abundantly throughout Müller cells, especially in the end feet at the inner limiting membrane, and in the photoreceptor outer segments and RPE layer (Figure 5). In the HFD-diabetic group, CRALBP immunofluorescence was also abundant in the photoreceptor outer segments but not in the Müller cell end feet at the inner limiting membrane. The C + AST group had a CRALBP immunofluorescent pattern similar to that observed in controls. In the HFD + AST-treated group, the CRALBP immunofluorescence in the Müller cell end feet was preserved and the expression pattern appeared similar to the controls.

Müller cell GS immunofluorescence was evaluated in retinal sections (Figure 6). Sections from control animals showed that Müller cell GS immunofluorescence was abundant in the INL and the retinal ganglion cell/nerve fiber layer, as well as processes spread between the inner limiting membrane and external limiting membrane. There was less GS immunofluorescence in sections from HFD-diabetic animals. GS immunoreactivity in controls fed with AST followed a similar pattern as that in the control group, while the HFD + AST group had diminished but still detectable GS immunoreactivity in the Müller cell projections and end-feet.

HFD diabetes promotes loss of retinal ganglion cell markers and synaptic vesicle protein in the retina of *P. obesus*

The transcription factor Brn3a is a specific marker of a subpopulation of retinal ganglion cells (Figure 7). In control animals, Brn3a immunofluorescence was detected in abundance in the cell bodies and nuclei of retinal ganglion cells. It was also detected to a lesser extent throughout the retinal tissue. In HFD-diabetic animals, the abundance of the retinal ganglion cells and the immunofluorescence intensity was reduced compared to control. The abundance and intensity

of Brn3a immunofluorescence in the HFD + AST animals was similar to that in the HFD group.

To assess the impact of HFD diabetes in *P. obesus* retinal synapses, we analyzed the marker of presynaptic neurotransmitter vesicles, synaptophysin (SVP 38), in control and HFD animals with and without AST treatment (Figure 8). In control gerbils, there was abundant synaptophysin immunofluorescence in both plexiform layers. Synaptophysin immunofluorescence was attenuated in the HFD-diabetic *P. obesus* group. Synaptophysin immunofluorescence in the C + AST group was comparable to that seen in the controls. Synaptophysin immunofluorescence in the HFD + AST group was also attenuated, similar to the HFD group (data not shown).

Discussion

Previously we demonstrated that AST was able to promote viability of *P. obesus* retinal cells under cytotoxic conditions.⁵⁷ In the present study, we tested the effects of HFD-induced obesity and diabetes on the expression of glial, neuronal, and synaptic markers in the retinas of *P. obesus*, and effects of short-term (7 days) AST administration 3 months after the onset of HFD. In previous studies, xanthophyll carotenoids were administered immediately after the onset of diabetes (4–7 days after streptozotocin (STZ) injection)^{50,58–60} as a long-term preventive strategy. The objective of this work was to determine whether AST could be effective in offsetting markers of diabetic retinal complications when administered later after the disease is fully established and diabetes-induced changes have already begun. Therefore, we only administered AST during the last seven days of the duration of the study.

Unlike the evolution of diabetes in other nutritionally induced models such as C57BL/6 J mice,⁶¹ Sprague–Dawley rats,⁶² and Wistar rats,⁶³ the onset of hyperglycemia in *P. obesus* occurs rapidly^{33,48,49} with a fast progression of diabetes-induced metabolic disorders.

The diet used in this study involved only minor modifications to a low-fat standard rodent diet. *P. obesus* developed obesity and hyperglycemia when held in captivity and fed with an enriched laboratory chow diet over 13 weeks, in agreement with previous reports that describe the genetic predisposition and metabolic syndrome of *P. obesus* when deprived from its natural habitat and diet.^{20,21,42,46} Therefore, the *P. obesus* gerbil is a replicable model of T2D when fed a hypercaloric diet in captivity.

Experimental studies linking HFD-induced obesity and prediabetes/diabetes to early retinal neurodegenerative features revealed that 3 months of HFD feeding regimen caused the onset of functional and morphological changes.^{45,61} Three-month *P. obesus* diabetic animals exhibited significantly delayed scotopic and photopic ERG responses (significant decrease of the amplitude of the b- and a-waves) and reduction of the amplitudes of scotopic oscillatory potentials after 3 months (Dellaa et al., unpublished data, 2018), suggesting that functional abnormalities were induced by the HFD.

The accumulation of advanced glycosylated end products is involved in the development and progression of microvascular diabetes-related disease as a result of chronic hyperglycemia.^{64,65}

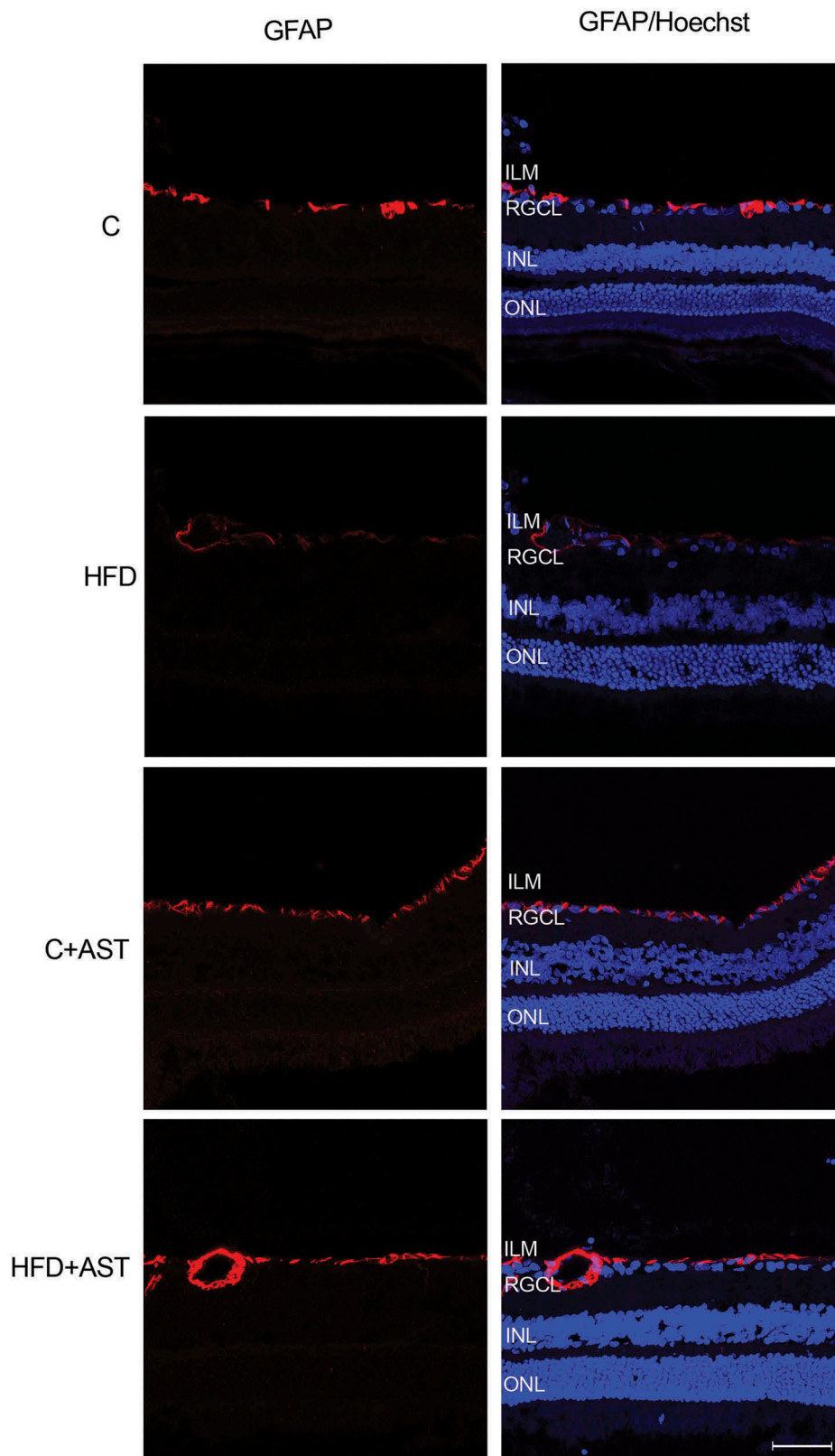


Figure 4. Absence of Müller cell reactivity in 13-week diabetic *Psammomys obesus* retinas to GFAP. GFAP-astrocytes immunostaining is restricted to the ILM in the HFD-diabetic *P. obesus* retinas. C, control; HFD, HFD-diabetic gerbils; C + AST, control treated with AST; HFD + AST, diabetic treated with AST. ILM, inner limiting membrane; RGCL, retinal ganglion cell layer; INL, inner nuclear layer; ONL, outer nuclear layer. Bar: 50 μ m.

Several clinical studies^{66–70} have identified a correlation between pentosidine plasma levels, severity of DR, and retinal hemodynamic abnormalities. During the early stages of NPDR, elevated pentosidine level has been found in diabetic patients.⁷¹ Our

results showed a significant increase in plasma pentosidine levels in 13-week diabetic animals.

The expression of HO-1 was altered in the HFD-diabetic *P. obesus*, being increased in the outer segments of the

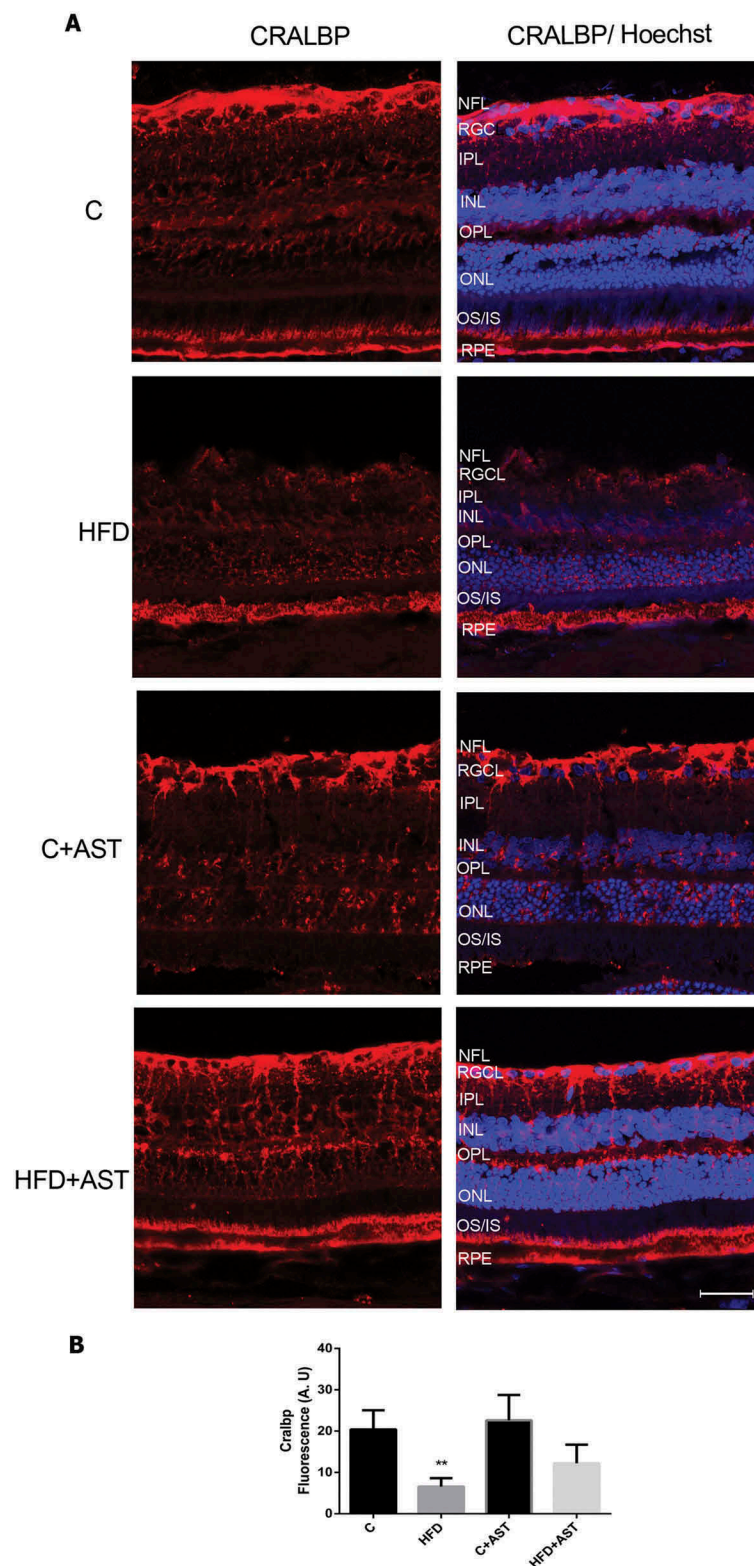


Figure 5. Astaxanthin ameliorates Müller cells CRALBP immunolabeling in HFD-diabetic *P. obesus* retinas. (A) CRALBP was labeled in C, controls; HFD, HFD-diabetic group; C + AST, controls treated with AST; HFD + AST, HFD-diabetic treated with AST. Cells nuclei were stained with Hoechst (blue). (B) Quantification of CRALBP immunofluorescence in treated and untreated control (black bars) and diabetic gerbils (gray bars). A.U., arbitrary units. ** $p < 0.01$ between control and diabetic. NFL, retinal nerve fiber layer; RGCL, retinal ganglion cell layer; IPL, inner plexiform layer; INL, inner nuclear layer; ONL, outer nuclear layer; IS/OS, inner and outer segments; RPE, retinal pigment epithelium. Bar: 50 μ m.

photoreceptors while decreased in the inner retina, compared to controls, and again the treatment with AST appeared to normalize this expression. Oxidative stress caused by hyperglycemia

plays a key role in the onset and progression of neuronal and vascular lesions in DR.^{72–75} HO-1 is considered a protective gene of the phase II detoxification enzymes, regulated by the

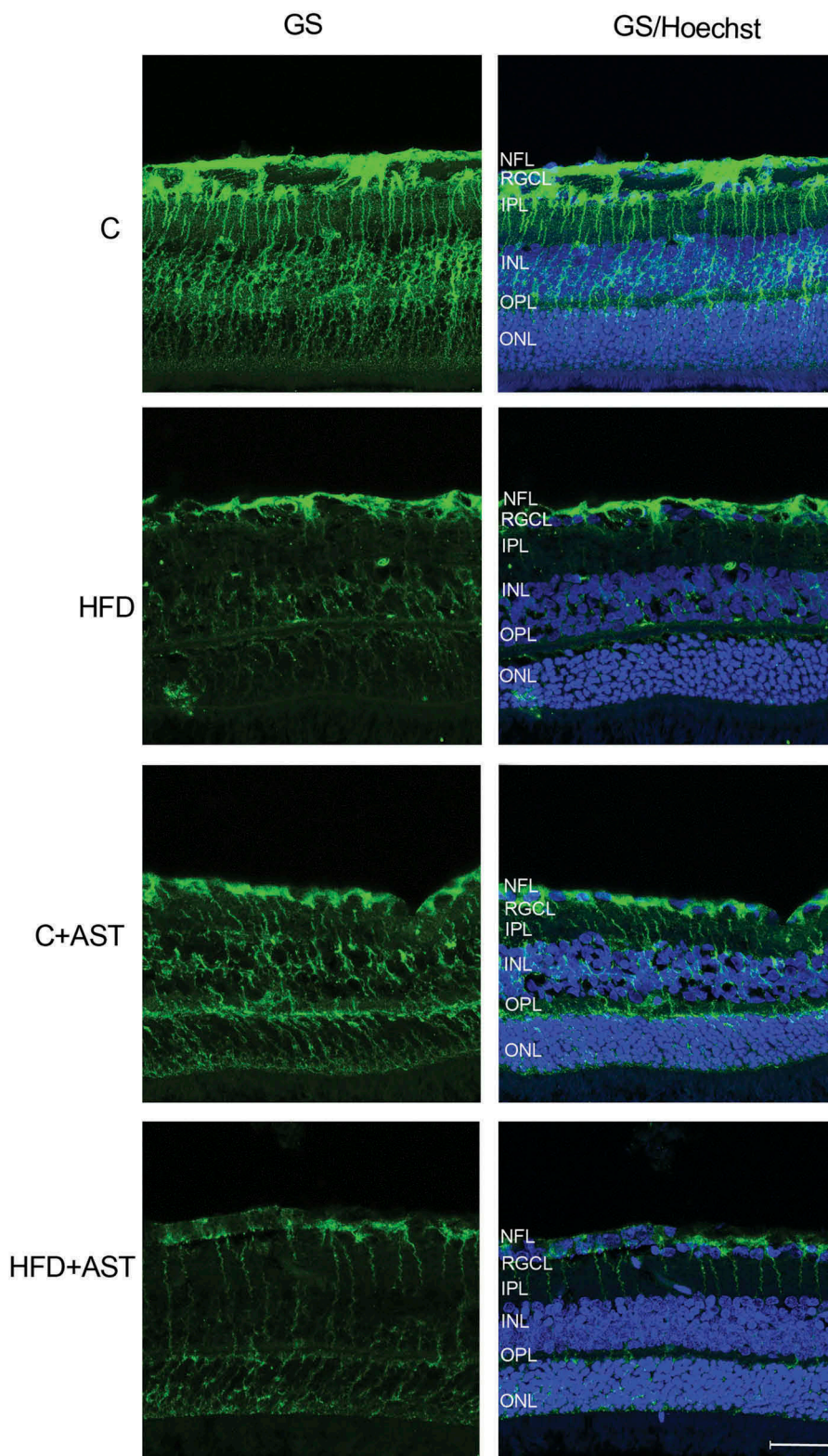


Figure 6. Short-term astaxanthin intake attenuated GS expression in the 13-week diabetic retinas of *P. obesus*. Immunostaining of anti-GS was performed in retina sections from C and HFD-diabetic animals as well as C + AST and HFD + AST groups. Cell nuclei were stained with Hoechst (blue). NFL, the retinal nerve fiber layer; RGCL, retinal ganglion cell layer; IPL, inner plexiform layer; INL, inner nuclear layer; ONL, outer nuclear layer. Bar: 50 μm .

antioxidant electrophile/antioxidant response element and the Nrf₂ transcription pathway.⁷⁶ HO-1 could be inducible under a variety of stress conditions (oxidative stress, inflammation) or pharmacological and antioxidant agents.^{77–80} After 4 weeks of

diabetes induction, the levels of expressed HO-1 protein and mRNA in rat retinal tissue were significantly higher than controls.⁸¹ The overexpression of HO-1 in photoreceptors in the *P. obesus* diabetic retina could be linked to oxidative stress

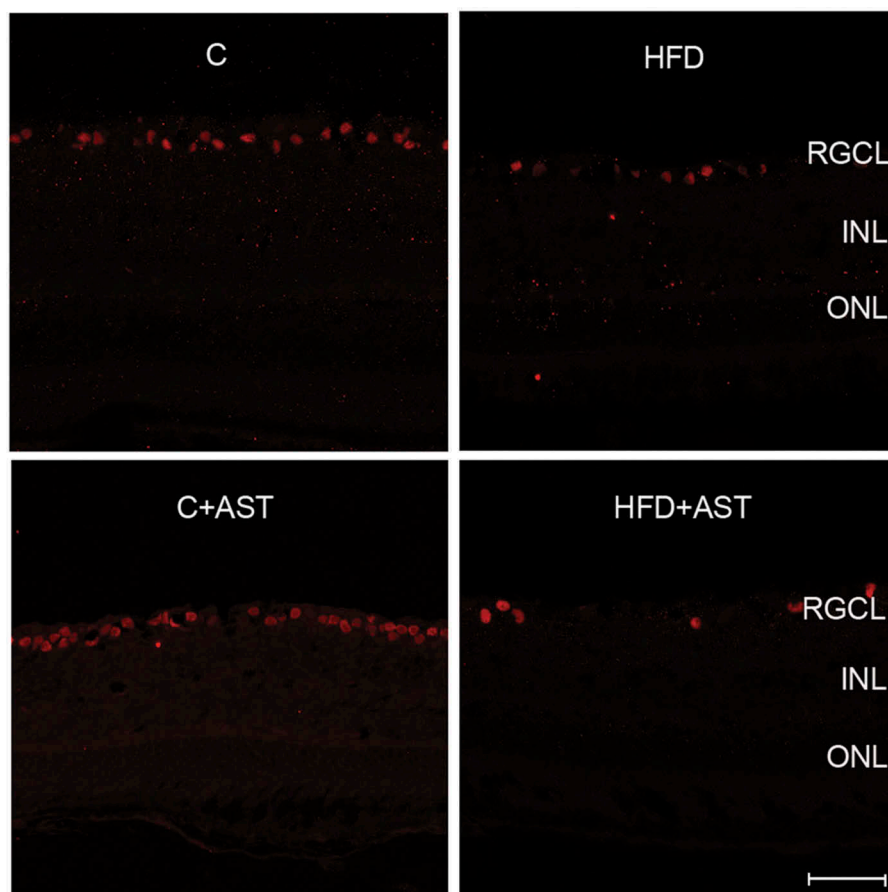


Figure 7. HFD-induced diabetes downregulated the expression of the transcription factor Brn3a. The Brn3a ganglion cells subpopulation was labeled in C, controls; HFD, diabetic animals; C + AST, control treated with AST. HFD + AST, diabetic treated with AST; RGCL, retinal ganglion cell layer; INL, inner nuclear layer; ONL, outer nuclear layer. Bar: 50 μ m.

since there is a high metabolic rate in this region of retina and is a likely source of oxidative stress.^{82–85}

In several reports, HO-1 protein expression was measured after the onset of disease, thus reflecting induced rather than basal HO-1 expression.⁸⁶ We noted higher basal HO-1 expression in control + AST gerbils. In a murine model of liver ischemia/reperfusion injury, basal rather than induced HO-1 protein levels were predictive of the antioxidant cytoprotection conferred by HO-1.⁸⁷ Carotenoids are able to induce the antioxidant defense system in diabetic conditions.⁷⁶ Mesozeaxanthin induced HO-1 levels in HFD-fed rat retina, whereas AST promoted NRF2 and increased the mRNA levels of HO-1 in STZ-diabetic retina.^{50,62} Accordingly, our qualitative results show that AST upregulated the expression of HO-1 in the RGCL, IPL, and photoreceptor outer segments in control and diabetic *P. obesus* retinas.

Astrocytes and Müller cells play key roles in the homeostasis of retina by providing structural and metabolic support to neurons and other cells.^{88–90} GFAP expression in astrocytes was reduced in the HFD-fed gerbils as observed in other diabetes animal models^{8,91} but there was no significant increase in expression in Müller cells, suggesting that the hyperglycemic condition induced by HFD is not acute enough to induce the extensive Müller cell reactivity observed in short-term diabetic animal models such as STZ-diabetic rats

or db/db mice. Similar results were observed in the retina of alloxan diabetic C57/Bl6 mice and STZ-diabetic Ins2Akita mice, where GFAP staining was mostly confined to astrocytes, similar to the controls.⁹² These differences may result from the diversity in animal strains and species.

Treatment with AST appeared to return the astrocytic expression of GFAP to control levels, suggesting that this acute antioxidant may reduce the inflammatory signals that alter astrocytic homeostasis in the retina. Similarly, AST increased the expression of CRALBP and GS in Müller cells of HFD-fed gerbils compared to controls, again suggesting that the acute anti-inflammatory influence of AST has a positive impact on multiple protein expression systems in both types of retinal macroglia.

The transcription factor Brn3a, exclusively expressed in RGC, regulates genes encoding for proteins necessary for survival/protection against apoptosis such as Bcl-2 and Bcl-XL.⁹³ HFD caused a significant reduction in the intensity of retinal ganglion cells, labeled by Brn3A. This result was as predicted since the majority of cell death would have occurred during the period before AST treatment. Our study cannot determine, therefore, whether or not AST is protective to retinal ganglion cells and other neurons of the inner retina; however, a preventive long-term AST administration protected retinal ganglion cells from diabetes-induced apoptosis in db/db mice,⁹⁴

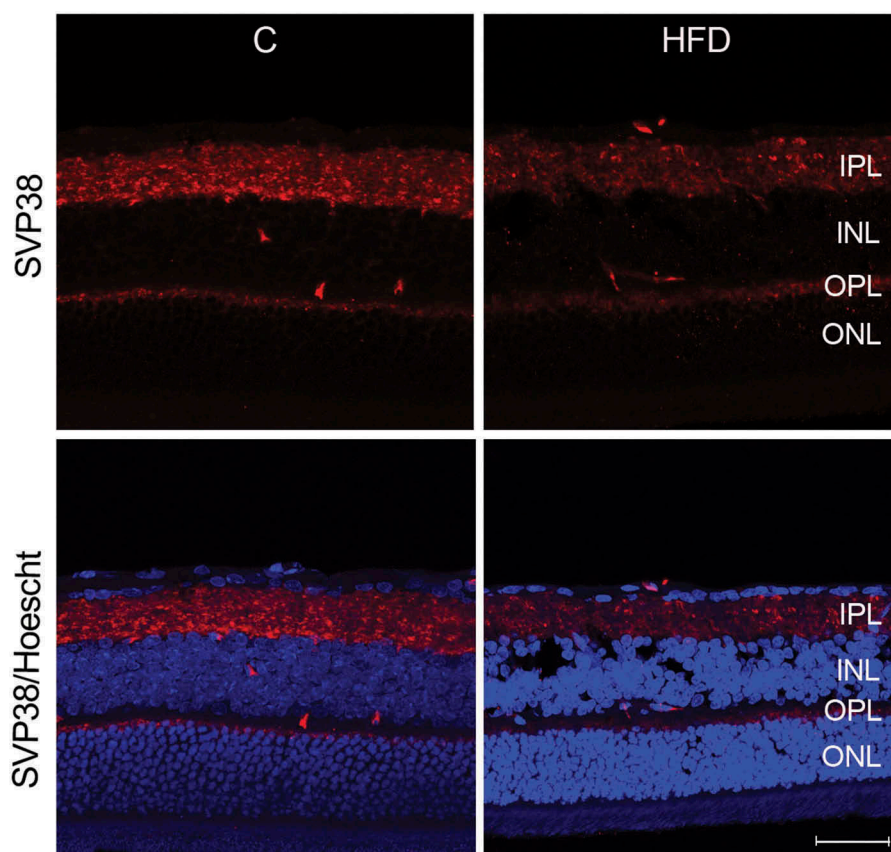


Figure 8. Representative photomicrographs of synaptophysin stained-retinal sections from C, control; HFD, diabetic. HFD-induced diabetes downregulated IPL synaptophysin signal. No evident differences in synaptophysin levels were observed in the AST-treated groups (data not shown). Cell nuclei were stained with Hoechst (blue). IPL, inner plexiform layer; INL, inner nuclear layer; ONL, outer nuclear layer. Bar: 50 μ m.

suggesting that AST could have been protective for RGCs in our study if administered during the entire duration of HFD.

Synaptophysin is a synaptic vesicle membrane glycoprotein expressed in neurons and used as a marker of synapses. The expression of SVP38 was reduced in the HFD-fed gerbils and did not recover with AST treatment, suggesting that this may also be a permanent deficit in gerbils after 3 months of diet-induced diabetes, although our data cannot rule out the possibility that a longer duration of AST treatment could rescue this reduction and that this morphological change is not reversible with a short duration of AST treatment, at least in animals that have experienced an extended period of hyperglycemia.

Conclusion

In summary, HFD-induced diabetes generally reduced the expression of glial markers GFAP, CRALBP, and GS. AST did also appear to increase the expression of the oxidative marker HO-1 and prevented glial changes from occurring. The short-time administration of AST did not rescue the expression of the retinal ganglion cell marker, Brn3a, and synaptophysin, a marker of presynaptic vesicles. Diabetic *P. obesus* is often associated with physiological and biological abnormalities in conjunction with disorders of lipid, carbohydrate, and vascular origin. *P. obesus* could be a useful experimental model to explore the implication of other diabetes risk

factors besides hyperglycemia in early retinal neurodegeneration mechanisms. Our qualitative study indicates that the carotenoid AST can confer a rapid antioxidant protective effect to the retina.

Acknowledgments

The authors thank Wei-Wei Wang for help with histology and immunofluorescence labeling in the Penn State College of Medicine. The assistance of Ons kesraoui (INRAP) during sample purification and Khoulood Hajri (ISBST) throughout HPLC assays is greatly appreciated. Astaxanthin (Sigma-Aldrich) was a kind gift of Serge Picaud and Valérie Fradot from the Institute of Vision of Paris, France. The authors also thank Professor Mohamed Hammami, Faculty of Medicine, University of Monastir, for the kind donation of standard pentosidine.

Declaration of interest

The authors confirm that there are no known conflicts of interest associated with this publication. The authors alone are responsible for the content and writing of the paper.

Funding

Part of this work was conducted in the framework of the Cross border project BIOVecQ, a program funded by the European Union through the IEVP program [Cod PS1.3_08 IEVP 2007-2013 Decision CE C (2008) 8275]. This work was also in part supported by the Wood Whelan Fellowship.

References

1. Schmidhuber J, Shetty P. The nutrition transition to 2030. Why developing countries are likely to bear the major burden. *Acta Agric Scand Sect C Food Econ.* 2005;2(3–4):150–66. doi:10.1080/16507540500534812.
2. Steyn NP, Mann J, Bennett PH, Temple N, Zimmet P, Tuomilehto J, Lindström J, Louheranta A. Diet, nutrition and the prevention of type 2 diabetes. *Public Health Nutr.* 2007;7(1a):147–65.
3. Katusic D, Tomic M, Jukic T, Kordic R, Sikic J, Vukojevic N, Saric B. Obesity—a risk factor for diabetic retinopathy in type 2 diabetes? *Coll Antropol.* 2005;29 Suppl 1:47–50.
4. Tataranni PA. Pathophysiology of obesity-induced insulin resistance and type 2 diabetes mellitus. *Eur Rev Med Pharmacol Sci.* 2002;6:27–32.
5. Eckel RH, Kahn SE, Ferrannini E, Goldfine AB, Nathan DM, Schwartz MW, Smith RJ, Smith SR. Obesity and type 2 diabetes: what can be unified and what needs to be individualized? *J Clin Endocrinol Metab.* 2011;96(6):1654–63. doi:10.1210/jc.2011-0585.
6. Garner A. Histopathology of diabetic retinopathy in man. *Eye.* 1993;7(2):250–53. doi:10.1038/eye.1993.58.
7. Barber AJ, Lieth E, Khin SA, Antonetti DA, Buchanan AG, Gardner TW. Neural apoptosis in the retina during experimental and human diabetes. Early onset and effect of insulin. *J Clin Invest.* 1998;102(4):783–91. doi:10.1172/JCI2425.
8. Aj B, Da A, Tw G; Group PSRR. Altered expression of retinal occludin and glial fibrillary acidic protein in experimental diabetes. *Invest Ophthalmol Vis Sci.* 2000;41(11):3561–68.
9. Martin PM, Roon P, Van Ells TK, Ganapathy V, Smith SB. Death of retinal neurons in streptozotocin-induced diabetic mice. *Invest Ophthalmol Vis Sci.* 2004;45(9):3330–36. doi:10.1167/iov.04-0247.
10. VanGuilder HD, Brucklacher RM, Patel K, Ellis RW, Freeman WM, Barber AJ. Diabetes downregulates presynaptic proteins and reduces basal synapsin I phosphorylation in rat retina. *Eur J Neurosci.* 2008;28(1):1–11. doi:10.1111/j.1460-9568.2008.06322.x.
11. Van Dijk HW, Verbraak FD, Kok PH, Stehouwer M, Garvin MK, Sonka M, DeVries JH, Schlingemann RO, Abramoff MD. Early neurodegeneration in the retina of type 2 diabetic patients. *Invest Ophthalmol Vis Sci.* 2012;53(6):2715–19. doi:10.1167/iov.11-8997.
12. Sohn EH, Van Dijk HW, Jiao C, Kok PH, Jeong W, Demirkaya N, Garmager A, Wit F, Kucukcilioglu M, Van Velthoven ME, et al. Retinal neurodegeneration may precede microvascular changes characteristic of diabetic retinopathy in diabetes mellitus. *Proc Natl Acad Sci U S A.* 2016;113(19):E2655–64. doi:10.1073/pnas.1522014113.
13. Thomas RL, Dunstan F, Luzio SD, Roy Chowdury S, Hale SL, North RV, Gibbins RL, Owens DR. Incidence of diabetic retinopathy in people with type 2 diabetes mellitus attending the Diabetic Retinopathy Screening Service for Wales: retrospective analysis. *BMJ.* 2012;344:1–11.
14. Fong DS, Aiello L, Gardner TW, King GL, Blankenship G, Cavallerano JD, Ferris FL, Klein R. Retinopathy in diabetes. *Diabetes Care.* 2004;27(suppl 1):s84–s7. doi:10.2337/diabetes.27.2007.S84.
15. Lee R, Wong TY, Sabanayagam C. Epidemiology of diabetic retinopathy, diabetic macular edema and related vision loss. *Eye Vis (Lond).* 2015;2:17. doi:10.1186/s40662-015-0026-2.
16. Chaabo F, Pronczuk A, Maslova E, Hayes K. Nutritional correlates and dynamics of diabetes in the Nile rat (*Arvicanthis niloticus*): a novel model for diet-induced type 2 diabetes and the metabolic syndrome. *Nutr Metab.* 2010;7(1):29. doi:10.1186/1743-7075-7-29.
17. Hammoum I, Mbarek S, Dellaa A, Dubus E, Baccouche B, Azaiz R, Charfeddine R, Picaud S, Ben Chaouacha-Chekir R. Study of retinal alterations in a high fat diet-induced type ii diabetes rodent: *Meriones shawi*. *Acta Histochem.* 2016;119(1):1–9.
18. Ventura LLA, Fortes NCL, Santiago HC, Caliari MV, Gomes MA, Oliveira DR. Obesity-induced diet leads to weight gain, systemic metabolic alterations, adipose tissue inflammation, hepatic steatosis, and oxidative stress in gerbils (*Meriones unguiculatus*). *PeerJ.* 2017;5:e2967. doi:10.7717/peerj.2967.
19. Noda K, Mark M, Souska Z, Sonja F, Faryan T, Shintaro N, Toshio H, Lama A, Anrzej P, Hayes KC, et al. An animal model of spontaneous metabolic syndrome: Nile grass rat. *FASEB J.* 2010. doi:10.1096/fj.09-152678.
20. Marquie G, Duhault J, Jacotot B. Diabetes Mellitus in Sand Rats (*Psammomys obesus*): Metabolic Pattern During Development of the Diabetic Syndrome. *Diabetes.* 1984;33(5):438–43.
21. Kaiser N, Cerasi E, Leibowitz G. Diet-induced diabetes in the sand rat (*Psammomys obesus*). In: Joost H-G, Al-Hasani H, Schürmann A, editors. *Animal models in diabetes research.* Totowa (NJ): Humana Press; 2012. p. 89–102.
22. Degen AA, Kam M, Khokhlova IS, Zeevi Y. Fiber digestion and energy utilization of fat sand rats (*Psammomys obesus*) consuming the chenopod *anabasis articulata*. *Physiol Biochem Zool.* 2000;73(5):574–80. doi:10.1086/317756.
23. Degen AA, Hazan A, Kam M, Nagy KA. Seasonal water influx and energy expenditure of free-living fat sand rats. *J Mammal.* 1991;72(4):652–57. doi:10.2307/1381826.
24. Kalman R, Ziv E, Lazarovic G, Shafir E. Sand rat. In: Suckow MA, Stevens KA, Wilson RP, editors. *The Laboratory Rabbit, Guinea Pig, Hamster, and Other Rodents.* San Diego, USA: Elsevier Academic Press; 2012.
25. Petter F, Lachiver F, Chekir R. Les adaptations des rongeurs Gerbillidés à la vie dans les régions arides. *Bulletin de la Société Botanique de France. Actualités Botaniques.* 1984;131(2–4):365–73. doi:10.1080/01811789.1984.10826676.
26. Gouaref I, Detaille D, Wiernsperger N, Khan NA, Leverve X, Koccir EA. The desert gerbil *Psammomys obesus* as a model for metformin-sensitive nutritional type 2 diabetes to protect hepatocellular metabolic damage: impact of mitochondrial redox state. *PLoS One.* 2017;12(2):e0172053. doi:10.1371/journal.pone.0172053.
27. El Aoufi S, Gendre P, Sennoune SR, Rigoard P, Maixent JM, Griene L. A high calorie diet induces type 2 diabetes in the desert sand rat (*Psammomys obesus*). *Cell Mol Biol (Noisy-Le-Grand).* 2007;53:O1943–53.
28. Marquie G, Duhault J, Jacotot B. Diabetes mellitus in sand rats (*Psammomys obesus*): metabolic pattern during development of the diabetic syndrome. *Diabetes.* 1984;33(5):438–43. doi:10.2337/diabetes.33.5.438.
29. Levy E, Lalonde G, Delvin E, Elchebly M, Precourt LP, Seidah NG, Spahis S, Rabasa-Lhoret R, Ziv E. Intestinal and hepatic cholesterol carriers in diabetic *Psammomys obesus*. *Endocrinology.* 2010;151(3):958–70. doi:10.1210/en.2009-0866.
30. Scherzer P, Katalan S, Got G, Pizov G, Londono I, Gal-Moscovici A, Popovtzer MM, Ziv E, Bendayan M. *Psammomys obesus*, a particularly important animal model for the study of the human diabetic nephropathy. *Anat Cell Biol.* 2011;44(3):176–85. doi:10.5115/acb.2011.44.3.176.
31. Sahaoui A, Dewachter C, De Medina G, Naeije R, Aouichat Bouguerra S, Dewachter L. Myocardial structural and biological anomalies induced by high fat diet in *Psammomys obesus* Gerbils. *PLoS One.* 2016;11(2):e0148117. doi:10.1371/journal.pone.0148117.
32. Spolding B, Connor T, Wittmer C, Abreu LL, Kaspi A, Ziemann M, Kaur G, Cooper A, Morrison S, Lee S, et al. Rapid development of non-alcoholic steatohepatitis in *Psammomys obesus* (Israeli sand rat). *PLoS One.* 2014;9(3):e92656. doi:10.1371/journal.pone.0092656.
33. Kaiser N, Neshar R, Donath MY, Fraenkel M, Behar V, Magnan C, Ktorza A, Cerasi E, Leibowitz G. *Psammomys obesus*, a model for environment-gene interactions in type 2 diabetes. *Diabetes.* 2005;54(Suppl 2):S137–44. doi:10.2337/diabetes.54.suppl_2.S137.
34. Saidi T, Mbarek S, Chaouacha-Chekir RB, Hicks D. Diurnal rodents as animal models of human central vision: characterisation of the retina of the sand rat *Psammomys obesus*. *Graefes Arch Clin Exp Ophthalmol.* 2011;249(7):1029–37. doi:10.1007/s00417-011-1641-9.
35. Dellaa A, Polosa A, Mbarek S, Hammoum I, Messaoud R, Amara S, Azaiz R, Charfeddine R, Dogui M, Khairallah M, et al. Characterizing the retinal function of *Psammomys obesus*: a

- diurnal rodent model to study human retinal function. *Curr Eye Res.* 2016;42(1):79–87. doi:10.3109/02713683.2016.1141963.
36. Dellaa A, Benlarbi M, Hammoum I, Gammoudi N, Dogui M, Messaoud R, Azaiz R, Charfeddine R, Khairallah M, Lachapelle P, et al. Electroretinographic evidence suggesting that the type 2 diabetic retinopathy of the sand rat *Psammomys obesus* is comparable to that of humans. *PLOS ONE.* 2018;13(2):e0192400. doi:10.1371/journal.pone.0192400.
 37. Saidi T, Mbarek S, Omri S, Behar-Cohen F, Chaouacha-Chekir RB, Hicks D. The sand rat, *Psammomys obesus*, develops type 2 diabetic retinopathy similar to humans. *Invest Ophthalmol Vis Sci.* 2011;52(12):8993–9004. doi:10.1167/iovs.11-8423.
 38. Saidi T, Ben Chaouacha-Chekir R, Hicks D. Advantages of *Psammomys obesus* as an animal model to study diabetic retinopathy. *J Diabetes Metab.* 2012;03(06). doi:10.4172/2155-6156.1000207.
 39. Soliman MK, Sadiq MA, Agarwal A, Sarwar S, Hassan M, Hanout M, Graf F, High R, Do DV, Nguyen QD, et al. High-resolution imaging of parafoveal cones in different stages of diabetic retinopathy using adaptive optics fundus camera. *PLoS One.* 2016;11(4):e0152788. doi:10.1371/journal.pone.0152788.
 40. Yamamoto S, Kamiyama M, Nitta K, Yamada T, Hayasaka S. Selective reduction of the S cone electroretinogram in diabetes. *Br J Ophthalmol.* 1996;80(11):973–75. doi:10.1136/bjo.80.11.973.
 41. Daly M, Daly S. On the feeding ecology of *Psammomys obesus* (Rodentia, Gerbillidae) in the Wadi Saoura, Algeria. *Mammalia.* 1973;37(4):545–61. doi:10.1515/mamm.1973.37.4.545.
 42. Bouguerra SA, Bourdillon MC, Dahmani Y, Bekkhoucha E. Non insulin dependent diabetes in sand rat (*Psammomys obesus*) and production of collagen in cultured aortic smooth muscle cells. Influence of insulin. *Int J Exp Diabetes Res.* 2001;2(1):37–46. doi:10.1155/EDR.2001.37.
 43. Ikeda Y, Olsen GS, Ziv E, Hansen LL, Busch AK, Hansen BF, Shafirir E, Mosthaf-Seedorf L. Cellular mechanism of nutritionally induced insulin resistance in *Psammomys obesus*. Overexpr Protein Kinase C α Skeletal Muscle Precedes Onset Hyperinsulinemia *Hyperglycemia.* 2001;50:584–92.
 44. Berrougui H, Ettaib A, Gonzalez MDH, Sotomayor M, Bennani-Kabchi N, Hmamouchi M. Hypolipidemic and hypocholesterolemic effect of argan oil (*Argania spinosa* L.) in *Meriones shawi* rats. *J Ethnopharmacol.* 2003;89(1):15–18. doi:10.1016/S0378-8741(03)00176-4.
 45. Hammoum I, Benlarbi M, Dellaa A, Szabo K, Dekany B, Csaba D, Almasi Z, Hajdu RI, Azaiz R, Charfeddine R, et al. Study of retinal neurodegeneration and maculopathy in diabetic *Meriones shawi*: A particular animal model with human-like macula. *J Comp Neurol.* 2017. doi:10.1002/cne.24245.
 46. Collier GR, Walder K, Lewandowski P, Sanigorski A, Zimmet P. Leptin and the development of obesity and diabetes in *Psammomys obesus*. *Obes Res.* 1997;5(5):455–58. doi:10.1002/j.1550-8528.1997.tb00670.x.
 47. Walder KR, Fahey RP, Morton GJ, Zimmet PZ, Collier GR. Characterization of obesity phenotypes in *Psammomys obesus* (Israeli sand rats). *Int J Exp Diabetes Res.* 2000;1(3):177–84. doi:10.1155/EDR.2000.177.
 48. Kaiser N, Yuli M, Üçkaya G, Oprescu AI, Berthault M-F, Kargar C, Donath MY, Cerasi E, Ktorza A. Dynamic changes in β -cell mass and pancreatic insulin during the evolution of nutrition-dependent diabetes in *Psammomys obesus*. *Impact Glycemic Control.* 2005;54:138–45.
 49. Leibowitz G, Yuli M, Donath MY, Neshet R, Melloul D, Cerasi E, Gross DJ, Kaiser N. Cell glucotoxicity in the *psammomys obesus* model of type 2 diabetes. *DIABETES.* 2001;50(1):S113–S7. doi:10.2337/diabetes.50.2007.S113.
 50. Yeh PT, Huang HW, Yang CM, Yang WS, Yang CH. Astaxanthin inhibits expression of retinal oxidative stress and inflammatory mediators in streptozotocin-induced diabetic rats. *PLoS One.* 2016;11(1):e0146438. doi:10.1371/journal.pone.0146438.
 51. DMS. Astaxanthin fact sheet Netherlands: DMS. 2014 [accessed 2014 Jan 21]. https://www.dsm.com/content/dam/dsm/foodandbeverages/en_US/documents/hnh/Astaxanthin-Fact-Sheet.pdf.
 52. Kerkeni M, Weiss IS, Jaisson S, Dandana A, Addad F, Gillery P, Hammami M. Increased serum concentrations of pentosidine are related to presence and severity of coronary artery disease. *Thromb Res.* 2014;134(3):633–38. doi:10.1016/j.thromres.2014.07.008.
 53. Scheijen JL, Van De Waarenburg MP, Stehouwer CD, Schalkwijk CG. Measurement of pentosidine in human plasma protein by a single-column high-performance liquid chromatography method with fluorescence detection. *J Chromatogr B Analyt Technol Biomed Life Sci.* 2009;877(7):610–14. doi:10.1016/j.jchromb.2009.01.022.
 54. Eidet JR, Pasovic L, Maria R, Jackson CJ, Utheim TP. Objective assessment of changes in nuclear morphology and cell distribution following induction of apoptosis. *Diagn Pathol.* 2014;9:92. doi:10.1186/1746-1596-9-92.
 55. Fernandez-Bueno I, Jones R, Soriano-Romaní L, López-García A, Galvin O, Cheetham S, Diebold Y. Histologic characterization of retina neuroglia modifications in diabetic Zucker Diabetic Fatty rats. *Invest Ophthalmol Vis Sci.* 2017;58(11):4925–33. doi:10.1167/iovs.17-21742.
 56. Feenstra DJ, Yego EC, Mohr S. Modes of retinal cell death in diabetic retinopathy. *J Clin Exp Ophthalmol.* 2013;4:298.
 57. Baccouche B, Mbarek S, Dellaa A, Hammoum I, Messina CM, Santulli A, Ben Chaouacha-Chekir R. Protective effect of astaxanthin on primary retinal cells of the Gerbil *Psammomys obesus* cultured in diabetic milieu. *J Food Biochem.* 2016;41(1):e12274-n/a. doi:10.1111/jfbc.12274.
 58. Sasaki M, Ozawa Y, Kurihara T, Kubota S, Yuki K, Noda K, Kobayashi S, Ishida S, Tsubota K. Neurodegenerative influence of oxidative stress in the retina of a murine model of diabetes. *Diabetologia.* 2010;53(5):971–79. doi:10.1007/s00125-009-1655-6.
 59. Kowluru RA, Menon B, Gierhart DL. Beneficial effect of zeaxanthin on retinal metabolic abnormalities in diabetic rats. *Invest Ophthalmol Vis Sci.* 2008;49(4):1645–51. doi:10.1167/iovs.07-0764.
 60. Muriach M, Bosch-Morell F, Alexander G, Blomhoff R, Barcia J, Arnal E, Almansa I, Romero FJ, Miranda M. Lutein effect on retina and hippocampus of diabetic mice. *Free Radic Biol Med.* 2006;41(6):979–84. doi:10.1016/j.freeradbiomed.2006.06.023.
 61. Chang RC-A, Shi L, Huang CC-Y, Kim AJ, Ko ML, Zhou B, Ko GYP. High-fat diet-induced retinal dysfunction high-fat diet-induced retinal dysfunction. *Invest Ophthalmol Vis Sci.* 2015;56(4):2367–80. doi:10.1167/iovs.14-16143.
 62. Orhan C, Akdemir F, Tuzcu M, Sahin N, Yilmaz I, Deshpande J, Juturu V, Sahin K. Mesozexanthin protects retina from oxidative stress in a rat model. *J Ocul Pharmacol Ther.* 2016;32(9):631–37. doi:10.1089/jop.2015.0154.
 63. Marcal AC, Leonelli M, Fiamoncini J, Deschamps FC, Rodrigues MA, Curi R, Carpinelli AR, Britto LR, Carvalho CR. Diet-induced obesity impairs AKT signalling in the retina and causes retinal degeneration. *Cell Biochem Funct.* 2013;31(1):65–74. doi:10.1002/cbf.2861.
 64. Goh SY, Cooper ME. Clinical review: the role of advanced glycation end products in progression and complications of diabetes. *J Clin Endocrinol Metab.* 2008;93(4):1143–52. doi:10.1210/jc.2007-1817.
 65. Kerkeni M, Saïdi A, Bouzidi H, Letaïef A, Yahia SB, Hammami M. Pentosidine as a biomarker for microvascular complications in type 2 diabetic patients. *Diabetes Vasc Dis Res.* 2013;10(3):239–45. doi:10.1177/1479164112460253.
 66. Ghanem AA, Elewa A, Arafat LF. Pentosidine and N-carboxymethyl-lysine: biomarkers for type 2 diabetic retinopathy. *Eur J Ophthalmol.* 2011;21(1):48–54. doi:10.5301/EJO.2010.4447.
 67. Hegab Z, Gibbons S, Neyses L, Mamas MA. Role of advanced glycation end products in cardiovascular disease. *World J Cardiol.* 2012;4(4):90–102. doi:10.4330/wjcv.v4.i4.90.
 68. Kerkeni M, Saïdi A, Bouzidi H, Ben Yahya S, Hammami M. Elevated serum levels of AGEs, sRAGE, and pentosidine in Tunisian patients with severity of diabetic retinopathy. *Microvasc Res.* 2012;84(3):378–83. doi:10.1016/j.mvr.2012.07.006.
 69. Ono Y, Aoki S, Ohnishi K, Yasuda T, Kawano K, Tsukada Y. Increased serum levels of advanced glycation end-products and diabetic complications. *Diabetes Res Clin Pract.* 1998;41(2):131–37. doi:10.1016/S0168-8227(98)00074-6.

70. Sato E, Nagaoka T, Yokota H, Takahashi A, Yoshida A. Correlation between plasma pentosidine concentrations and retinal hemodynamics in patients with type 2 diabetes. *Am J Ophthalmol.* 2012;153(5):903–9.e1. doi:10.1016/j.ajo.2011.10.020.
71. Salman AG, Mansour DE, Swelem AH, Al-Zawahary WM, Radwan AA. Pentosidine - a new biochemical marker in diabetic retinopathy. *Ophthalmic Res.* 2009;42(2):96–98. doi:10.1159/000225661.
72. Kowluru RA, Chan PS. Oxidative stress and diabetic retinopathy. *Exp Diabetes Res.* 2007;2007:43603. doi:10.1155/2007/43603.
73. Shin ES, Huang Q, Gurel Z, Sorenson CM, Sheibani N. High glucose alters retinal astrocytes phenotype through increased production of inflammatory cytokines and oxidative stress. *PLoS One.* 2014;9(7):e103148. doi:10.1371/journal.pone.0103148.
74. Du Y, Smith MA, Miller CM, Kern TS. Diabetes-induced nitrate stress in the retina, and correction by aminoguanidine. *J Neurochem.* 2002;80(5):771–79. doi:10.1046/j.0022-3042.2001.00737.x.
75. Kowluru RA, Mishra M. Oxidative stress, mitochondrial damage and diabetic retinopathy. *Biochim Biophys Acta.* 2015;1852(11):2474–83. doi:10.1016/j.bbadis.2015.08.001.
76. Ben-Dor A, Steiner M, Gheber L, Danilenko M, Dubi N, Linnewiel K, Zick A, Sharoni Y, Levy J. Carotenoids activate the antioxidant response element transcription system. *Mol Cancer Ther.* 2005;4:175–89.
77. Said L, Fabienne T, Antony L, Carole B, Puy H, Jean-Pierre L. Protective role of heme oxygenase and heme catabolites. *Hématologie (Montrouge).* 2007;13:251–64.
78. Ulyanova T, Szel A, Kutty RK, Wiggert B, Caffè AR, Chader GJ, Van Veen T. Oxidative stress induces heme oxygenase-1 immunoreactivity in Muller cells of mouse retina in organ culture. *Invest Ophthalmol Vis Sci.* 2001;42:1370–74.
79. Abraham NG, Kappas A. Pharmacological and clinical aspects of heme oxygenase. *Pharmacol Rev.* 2008;60(1):79–127. doi:10.1124/pr.107.07104.
80. Ndisang JF, Lane N, Syed N, Jadhav A. Up-regulating the heme oxygenase system with hemin improves insulin sensitivity and glucose metabolism in adult spontaneously hypertensive rats. *Endocrinology.* 2010;151(2):549–60. doi:10.1210/en.2009-0471.
81. Fan J, Xu G, Jiang T, Qin Y. Pharmacologic induction of heme oxygenase-1 plays a protective role in diabetic retinopathy in rats. *Invest Ophthalmol Vis Sci.* 2012;53(10):6541–56. doi:10.1167/iops.11-9241.
82. Kern TS, Berkowitz BA. Photoreceptors in diabetic retinopathy. *J Diabetes Investig.* 2015;6(4):371–80. doi:10.1111/jdi.12312.
83. Du Y, Veenstra A, Palczewski K, Kern TS. Photoreceptor cells are major contributors to diabetes-induced oxidative stress and local inflammation in the retina. *Proc Natl Acad Sci U S A.* 2013;110(41):16586–91. doi:10.1073/pnas.1314575110.
84. Sun M-H, Pang J-HS, Chen S-L, Kuo P-C, Chen K-J, Kao L-Y, Wu J-Y, Lin -K-K, Tsao Y-P. Photoreceptor protection against light damage by AAV-mediated overexpression of heme oxygenase-1. *Invest Ophthalmol Vis Sci.* 2007;48(12):5699–707. doi:10.1167/iops.07-0340.
85. Shyong MP, Lee FL, Hen WH, Kuo PC, Wu AC, Cheng HC, Chen SL, Tung TH, Tsao YP. Viral delivery of heme oxygenase-1 attenuates photoreceptor apoptosis in an experimental model of retinal detachment. *Vision Res.* 2008;48(22):2394–402. doi:10.1016/j.visres.2008.07.017.
86. Doberer D, Haschemi A, Andreas M, Zapf TC, Clive B, Jeitler M, Heinzl H, Wagner O, Wolzt M, Bilban M. Haem arginate infusion stimulates haem oxygenase-1 expression in healthy subjects. *Br J Pharmacol.* 2010;161(8):1751–62. doi:10.1111/j.1476-5381.2010.00990.x.
87. Tsuchihashi S, Livhits M, Zhai Y, Busuttill RW, Araujo JA, Kupiec-Weglinski JW. Basal rather than induced heme oxygenase-1 levels are crucial in the antioxidant cytoprotection. *J Immunol.* 2006;177(7):4749–57. doi:10.4049/jimmunol.177.7.4749.
88. Kolb H. Glial cells of the Retina. *Webvision, university of Utah, 2013, Web.* <http://webvision.med.utah.edu/book/part-ii-anatomy-and-physiology-of-the-retina/glia-cells-of-the-retina/>
89. Reichenbach A, Bringmann A. Müller cells in the Healthy Retina. *New York, NY: Springer; 2010.* p. 35–214.
90. Sorrentino FS, Allkabet M, Salsini G, Bonifazzi C, Perri P. The importance of glial cells in the homeostasis of the retinal microenvironment and their pivotal role in the course of diabetic retinopathy. *Life Sciences.* 2016;162:54–59. doi:10.1016/j.lfs.2016.08.001.
91. Barber AJ, Antonetti DA, Kern TS, Reiter CE, Soans RS, Krady JK, Levison SW, Gardner TW, Bronson SK. The Ins2Akita mouse as a model of early retinal complications in diabetes. *Invest Ophthalmol Vis Sci.* 2005;46(6):2210–18. doi:10.1167/iops.04-1340.
92. Gaucher D, Chiappore JA, Paques M, Simonutti M, Boitard C, Sahel JA, Massin P, Picaud S. Microglial changes occur without neural cell death in diabetic retinopathy. *Vision Res.* 2007;47(5):612–23. doi:10.1016/j.visres.2006.11.017.
93. Farooqui-Kabir SR, Budhram-Mahadeo V, Lewis H, Latchman DS, Marber MS, Heads RJ. Regulation of Hsp27 expression and cell survival by the POU transcription factor Brn3a. *Cell Death Differ.* 2004;11(11):1242–44. doi:10.1038/sj.cdd.4401478.
94. Dong LY, Jin J, Lu G, Kang XL. Astaxanthin attenuates the apoptosis of retinal ganglion cells in db/db mice by inhibition of oxidative stress. *Marine Drugs.* 2013;11:960–74. doi:10.3390/md11030960.